JOURNAL OF MATERIALS SCIENCE: MATERIALS IN MEDICINE **16** (2005) 775–781

Processing of an apatite-mullite glass-ceramic and an hydroxyapatite/phosphate glass composite by selective laser sintering

J. C. LORRISON[1], K. W. DALGARNO[1], D. J. WOOD[2]
[1]School of Mechanical Engineering and [2]Leeds Dental Institute, University of Leeds, Leeds, LS2 9JT, UK

The work presented details the results of an investigation into the feasibility of using Selective Laser Sintering (SLS) to directly produce customised bioceramic implants. The materials used were bioactive in nature and included a glass-ceramic and a combination of hydroxyapatite and phosphate glass. The glass-ceramic was selected from the range of apatite-mullite materials in the $SiO_2{\cdot}Al_2O_3{\cdot}CaO{\cdot}CaF_2{\cdot}P_2O_5$ series, due to their potentially suitable biological and mechanical properties. The hydroxyapatite and phosphate glass combination was chosen to allow an alternative production approach to be investigated. The viability of using both these materials with the SLS process was assessed and the process route and resulting material properties characterised using a variety of techniques including Differential Thermal Analysis (DTA), X-ray Diffraction (XRD) and Scanning Electron Microscopy (SEM).

The results obtained indicate that it was possible to produce multiple layer components from both materials using the SLS process. The glass-ceramic materials could only be processed at very low scan speeds and powers, yielding relatively brittle components. It was though possible to produce parts from the hydroxyapatite and phosphate glass combination across a much wider range of parameters, producing parts which had a greater potential for possible implant production.

1. Introduction

1.1. Background

Orthopaedic implants are commonly constructed from biologically nearly inert materials including metals (stainless steel, titanium alloys), ceramics (alumina, zirconia) and polymers (UHMWPE). A significant problem with many implants is the difficulty encountered when attempting to achieve a secure attachment between the implant and the surrounding bone tissue [1]. Implants are conventionally secured by bone cement, which can become loose after a period and also has the potential for inducing thermal necrosis as it sets through an exothermic reaction [2]. Depending on the application, implants may also be attached with pins or screws, which require further skeletal invasion and can act as stress concentrators.

There is therefore a case for creating implants from materials that can be attached by a more satisfactory method. Bioactive materials containing an apatite phase offer an attractive alternative as they can react to form a secure physical bond with tissue surrounding the implantation site. They can also be tailored to have similar mechanical properties to human bone [3]. This offers the advantages of a more secure attachment upon implantation than conventional implants and may also reduce the risk of stress shielding that relatively stiff metals can produce [1].

A further drawback of current implant technology is that a significant degree of skeletal adaptation is generally required to suit the chosen device, as skeletal morphology can vary significantly from patient to patient [4]. The economies of scale associated with conventional manufacturing processes lead to a limited range of implants for surgeons to choose from and as a result it is often simpler to modify the implant site than the implant itself. An obvious drawback of these restrictions is the degree of trauma inflicted upon the implant recipient and the related difficulties encountered in recuperation. It would therefore be highly desirable to have a process that would allow an implant to be produced which could be custom designed and built to suit individual cases. The aim of the work reported in this paper was to investigate the use of the selective laser sintering process with bioceramic materials to fabricate bone replacement implants which could be tailored to suit individual patient morphology.

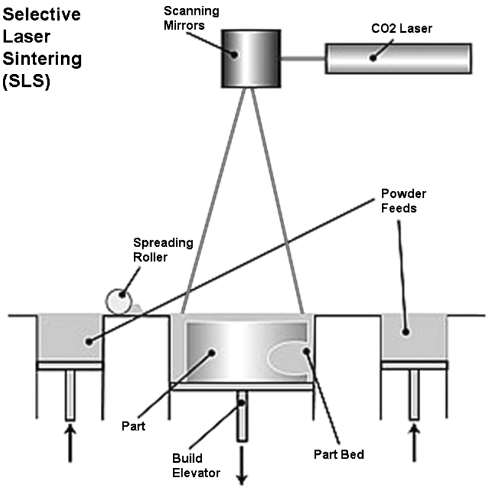

Figure 1 The selective laser sintering process [7].

1.2. Customised implant production via selective laser sintering

The ability to produce medical models from CAT scans via rapid prototyping techniques has been established for some time [5]. Such models however have largely been used for surgical procedure planning, being constructed from polymeric materials, and allow surgeons to see a physical model of a patient's anatomy prior to any operational procedure. Using the same techniques with bioceramics may allow custom built implants to be constructed that accurately map to individual patients, reducing the degree of trauma during surgery and thus potentially increasing patient survival rates. The focus of the work presented here has been to investigate the potential of such an approach.

The rapid prototyping technique used in this investigation was that of selective laser sintering, which is ideally suited to the production of parts from powdered materials, such as the pulverised glasses under analysis [6]. In the SLS process a layer of powder is spread over the working section of the sinter station by either a roller or hopper mechanism. The surface of the powdered material is then selectively scanned by a laser that provides enough energy to raise the temperature of the powder being scanned to above its melting point, fusing together those areas defined by the geometry of the section under construction. Once a layer has been scanned, the bed of the machine is lowered by an elevator platform to the thickness of one layer. A fresh layer of powder is then spread out and as the process is repeated the laser fuses together the subsequent layers creating a complete three-dimensional object. As Fig. 1 shows, the unfused powder provides support for isolated structural components as they are fabricated.

In this research project an experimental sinter station was used, which comprises two 125 Watt CO_2 lasers combined to produce a total power output of 250 Watts. The basic layout of the machine is shown in Fig. 2, and further details of the machine are described by Lorrison [8].

1.3. Apatite-mullite glass-ceramics

The initial premise upon which the criteria for material selection was based focused on the bioactivity of the glass-ceramic. It was decided that this should come from an apatite phase, and is known to exist in three basic material groups. These are the ceramic hydroxyapatite and the glass-ceramics apatite-wollastonite (A-W) and apatite-mullite (A-M). Of these materials it is known that hydroxyapatite degrades at the high temperatures needing for sintering, whilst A-W and A-M may have a greater processing potential [10]. In this case the A-M range was selected for initial investigation.

Apatite-mullite glass-ceramics derive their strength from a crystal structure of fine interlocking acicular crystals that give a greater mechanical strength than is seen in the base glass alone [11]. The final choice of material came from a variant within the A-M range, which was thought to have sufficient bioactivity and satisfactory mechanical properties.

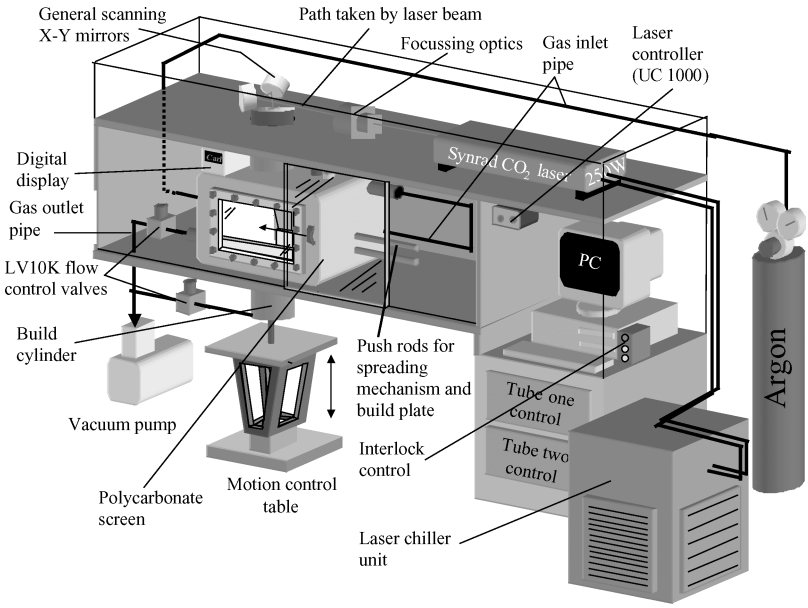

Figure 2 Experimental sinterstation layout [9].

1.4. Hydroxyapatite and phosphate glass

In addition to investigating SLS of a single material an alternative approach was also investigated. Previous work using conventional sintering techniques had shown that it was possible to produce biomedical implants from a composite of hydroxyapatite and resorbable phosphate glass. Tancred reported that, by using phosphate glass additions of up to 10% by weight with hydroxyapatite, there was a significant enhancement in the composite strength of up to 200% when compared to that of hydroxyapatite alone [12].

The reasons for using a similar composition with the laser sintering process are twofold: firstly such an approach had been shown to yield results that had the potential to produce useable bioactive implants. Secondly, and perhaps equally as important, is that a biphasic approach which mimics the indirect laser sintering approach may allow greater flexibility in the processing regime than is afforded by the use of just one material. The indirect process mixes a material that has a relatively high melting temperature with a lower melting temperature binder, often a thermoplastic, which allows a whole green part to be formed without needing to heat the entire build section [6]. After laser sintering the green part is post-processed to burn off the binder and to sinter the higher melting temperature material, yielding the final product. Subject to any finishing processes the part is then ready for use.

Analogous to this process is the use of a relatively low melting temperature phosphate glass, as a semi-permanent binder, in combination with hydroxyapatite as the solid phase. The phosphate glass should hold the hydroxyapatite together, to create a suitably strong implantable material, before being resorbed by the body upon implantation to allow the ingrowth and attachment of bone tissue to the remaining hydroxyapatite structure.

2. Materials and methods

2.1. Formation of the glass-ceramic

A glass was made according to the formula:

$$4.5SiO_2{\cdot}3Al_2O_3{\cdot}1.6P_2O_5{\cdot}3CaO{\cdot}2CaF_2$$

The components required for production of the glass were weighed separately on a balance and placed in a container with an agitating bar for mixing in a rotary mill. After an hour the mixture was transferred to a mullite crucible and placed in a furnace at 1450 °C for 2 h, being brought out briefly after an hour to be swirled around to aid homogenisation. The crucible was then removed from the furnace and the molten glass shock quenched by pouring directly into water with sufficient speed to prevent crystallisation. Once cooled, the glass was dried before being pulverised with a 250 ml puck-and-ring mill in a Gy-Ro Rotary Mill for approximately 120 seconds. The powdered material was then placed in a sieve stack and shaker (Octagon Digital) to separate it into the particle ranges 0–45, 45–90, 90–125 and 125 μm and above.

Fluorine loss is a major problem in any fluorine containing glasses and to ensure that glass of the required composition could be reproduced over several batches, three batches were made. The glass frit was examined by DTA to identify the glass transition temperature (T_g) and peak crystallisation temperatures (T_{pn}) [$n = 1$, 2, etc.] of any phases that would evolve during processing. T_g in particular is sensitive to fluorine loss, which might also ultimately affect the amount and type of any crystal phases present.

2.2. Hydroxyapatite and phosphate glass preparation

Whilst the hydroxyapatite (HA) was provided by a commercial supplier (Plasma Biotal Ltd.), the phosphate glass was produced specifically for this project from a formula provided by the Eastman Dental Institute at the University College of London [13]. It was chosen from the range of glasses in the series $P_2O_5{\cdot}CaO{\cdot}Na_2O$, as this would allow the desired characteristics of resorption, melting temperature and strength to be controlled. The phosphate glass used in this work (CNP) was essentially produced by the procedure described above for the A-M glass. The primary differences this time were the temperature of fusion, which was reduced to 1100 °C, and the method by which the glass was cooled. As phosphate glasses can react strongly with moisture it was not possible to shock quench by pouring the melt directly into water. To overcome this limitation it was decided to follow the protocol established by the Eastman Dental Institute for this glass and to pour the molten glass directly onto a steel plate, which was initially at room temperature. The combination of the large thermal mass of the plate, which was able to absorb the majority of the thermal energy of the glass relatively quickly, and the fluidity of the glass, which allowed it to spread quite thinly over the surface of the plate, allowed the glass to cool with a speed sufficient to prevent crystallisation. Once cooled the glass was processed to a sub 20 μm particle size and stored in a desiccater before being mixed with the hydroxyapatite in proportions varying from 2.5–20% (CNP:HA).

2.3. Selective laser sintering

In determining the viability of using bioceramic materials with the SLS process, a range of parameters may be altered. While the laser beam spot diameter was kept constant at 1.1 mm, the margin of overlap between subsequent lines, scan speed of the laser and laser power were all varied. To produce a single layer the laser scans a series of overlapping lines, which build up to produce a whole layer or *monolayer*. Each material and range of particle sizes was therefore tested by attempting to build monolayers across a range of the parameters described.

For the apatite-mullite material the scan speed was varied from 1–7 mm/s, while the laser power ranged from 0–10 W and the degree of line overlap was varied from 1/4, 1/2 and 3/4 of the beam width. To understand the processes occurring during the sintering cycle, it was necessary to determine the effect the heating regime had on the material in order that any

crystallisation processes might be identified. To achieve this the monolayers were analysed by DTA and XRD, which allowed the specific crystal phases to be identified and SEM, which provided an insight into the structural makeup of the parts.

For the hydroxyapatite and phosphate glass mixture the scan speed was varied from 1–500 mm/s, while the laser power ranged from 0–250 W and the degree of line overlap was again varied from 1/4, 1/2 and 3/4 of the beam width. In this instance, however, it was considered that little information could be derived by either DTA or XRD as the crystal structure of the primary HA component was already known. It was therefore decided to analyse the produced parts by visual inspection, physical handling and SEM.

After the basic processing route for creating monolayers had been established the construction of multiple layer parts was undertaken. This used the same parameters for producing monolayers while introducing the need to vary the layer thickness, which was controlled, as described previously, by the distance that the working section of the sinter station was lowered. With the equipment used the minimum layer thickness which could reliably be produced was 0.25 mm.

3. Results and discussion

3.1. Apatite-mullite glass-ceramic

The results of DTA runs on three batches of glass of the same nominal composition can be seen in Fig. 3. It may be seen from these traces that the glass transition temperature, T_g, of all three batches occurred at approximately 620 °C, whilst the first peaks (T_{p1}), corresponding to the crystallisation of the fluoroapatite phase, occurred at approximately 720 °C. The second peaks (T_{p2}), representing the mullite phase, tended to be in the same range (880–1020 °C) while the areas under the peaks showed a good correlation and gave an indication of the level of crystallisation. Due to the similarity in values for T_g and T_{p1}, the materials were characterised as having the same composition, as fluorine loss would have affected cross link density and hence T_g in particular [14]. The various particle size fractions were then blended together for subsequent SLS trials.

Of the particle size ranges used only the 0–45 μm and a mix of 0–45 μm and 45–90 μm ranges in a 1:1 ratio, produced useful results across a very narrow power range of 2–3 W and only with the 1/2 and 3/4 scan line overlaps. Table I describes the degree of coherence observed for a typical experiment across a range of laser scan speeds. It may be seen that while the processing window for producing coherent monolayers from the chosen material was very small, valid parts could be still be produced at low powers and scan speeds. An image of a complete part is displayed in Fig. 4 where the direction of the scan lines can be clearly seen.

TABLE I Degree of coherence for the 0–45 and 0–45:45–90 μm particle size ranges

Scan speed (mm/sec)		Material appearance
1		Satisfactory coherence
2	↓	Decreasing coherence
3		
....		
$3+n$		Little or no coherence

A typical DTA trace for the material after sintering can be seen in Fig. 5 and clearly shows that the peak representing the first phase had been almost completely removed. This indicated that the apatite phase crystallised out during the sintering process, possibly because the Ca:P ratio within this glass was close to that of the apatite stoichiometry. This meant that the driving force for this crystallisation may have been low compared to a sample with a Ca:P ratio further away from 1.67. It may also be observed, however, that the secondary phase remains almost completely unchanged. Hence there would be a need for heat treatment post-processing regimes to evolve this phase to gain the improved mechanical properties induced by mullite crystallisation [11].

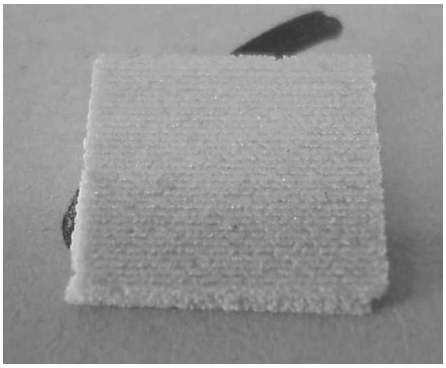

Figure 4 A multilayer components of LDIG105.

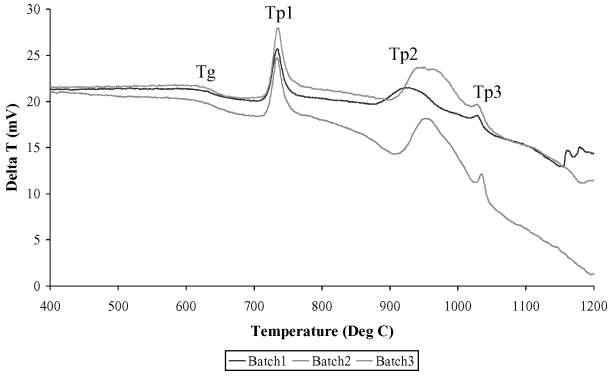

Figure 3 DTA traces of three batches of LDIG105.

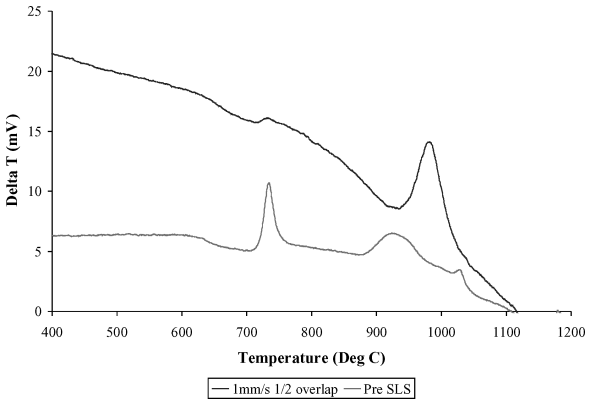

Figure 5 DTA traces of LDIG105 prior to and after laser sintering.

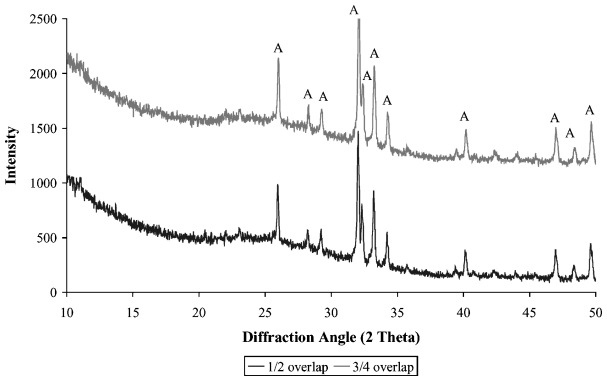

Figure 6 XRD traces of LDIG105 after laser sintering (A represents fluoroapatite).

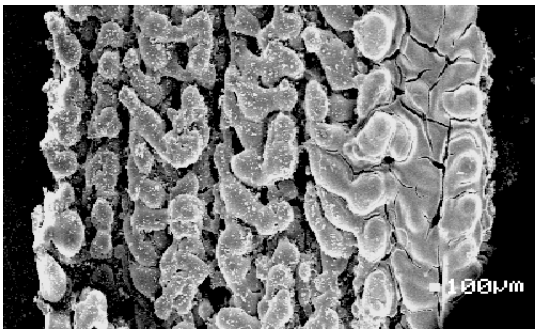

Figure 7 An SEM micrograph of an LDIG105 monolayer.

The phases seen in the scanned parts were identified by an XRD trace of the same monolayer, which may be seen in Fig. 6. This confirms that the crystallised material was essentially fluoroapatite, with very small amounts of mullite and aluminium phosphate.

Viewing a typical monolayer by SEM shows in detail the lines along which the laser scanned (see Fig. 7). While the reflective surface of the sample prevented visualisation of the interior microstructure of the monolayers it was an indication that a liquid phase must have been present during the sintering process. With conventional liquid phase sintering, sintering only occurs when two material phases are present [15]. This is because sintering usually occurs by heating an entire volume of material to a set temperature. In liquid phase sintering this would be high enough to melt one phase but not the other, resulting in a molten phase filling the voids around a solid phase creating a coherent body of material.

In the laser sintering process, however, sintering occurs only at the point where the laser makes contact with the surface of the powder bed. This can mean that only the smaller particles or those particles on the surface of the powder bed receive a sufficient quantity of thermal energy to cause them to melt. Once molten these particles form a liquid phase that occurs along with a solid phase, thus it may be said to be liquid phase sintering. This liquid phase may then be drawn down into the powder bed by capillary action or move around solid particles through the effects of surface tension. This gives a final material that is effectively liquid phase sintered as it contains a solid phase in particle form and a phase consisting of molten particles.

When the presence of liquid phase sintering is combined with the relatively highly porous powder bed it is reasonable to assume that a significant degree of densification has occurred during laser sintering. This is presumably the cause of the large separation that is evident between the lines. From the micron bar in the image it may be seen that the distance between the centres of the adjacent lines is approximately 200 μm or 0.2 mm. It is assumed that, as the laser scanned the first line of the layer onto the powder surface, the majority of the powder transiently melted to form a liquid phase. The nature of the porosity in the bed then must have caused the liquid phase material to migrate towards the centre of the line leaving vacant space on either side.

As the quantity of powder scanned by the laser in the next line is therefore only likely to be relatively small, it may be the case that when it melts, it forms the narrow lines seen, which in the same manner densify and shrink to form lines with vacant space around them. When subsequent lines are then scanned the process is effectively repeated, as the laser will not in fact be overlapping the previous lines in the assumed manner, due to the shrinkage and solidification of that line, and will rather be scanning partly vacant space, as well as the powder bed. Furthermore, the freshly scanned powder is presumably too far removed from the previous lines to bridge the space and attach to it. These factors, in combination with the knowledge that the previous line must already have solidified by the time the laser attempts to partly rescan it, make bonding between lines prohibitive as there is unlikely to be enough energy to remelt the previous line, even if it remained under the path of the laser, rather than migrating away from it. This would therefore account for the succession of apparently separate lines that may be observed.

The separation of the scan lines would also explain the relatively brittle nature of the monolayers produced, as there appears to be little connection between the lines and they may in fact only be held together by a small amount of liquid phase material that has been drawn down slightly into the powder bed by capillary action. When this is combined with the generally brittle nature of glasses, it is perhaps not surprising that the single layer scans are so friable.

A typical multiple layer part is shown in Fig. 4, where the individual layers, spread at a thickness of 0.25 mm, can be seen. It was seen that the multiple layer components showed similar fragility to the monolayers and so efforts were made to improve the mechanical properties of the components by using various heat treatment post-processing routes in order to consolidate the parts (see Table II for details). However, little or no improvement

TABLE II Post-processing regimes used with laser sintered LDIG105 components

Regime	Temperature profile	Heating rate
1	0–630 °C, hold for one hour, 630–1000 °C, hold for one hour	2 °C/min
2	0–1200 °C, hold for one hour	10 °C/min
3	0–1350 °C, hold for one hour	15 °C/min
4	0–1430 °C, hold for one hour	15 °C/min

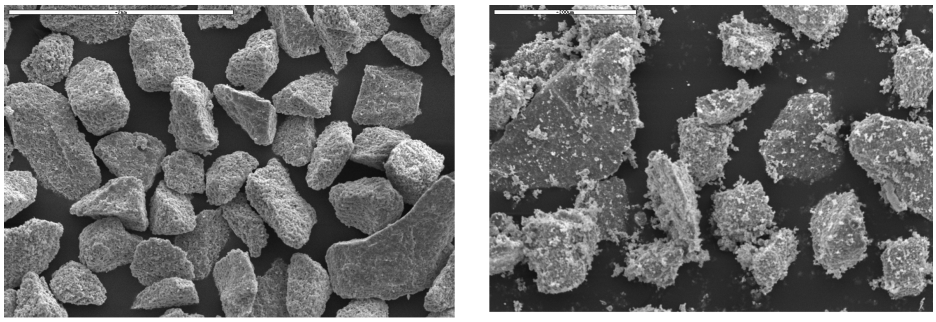

(a) (b)

Figure 8 SEM micrographs of (a) pure HA particles; (b) a blend of HA and phosphate glass.

could be made to the cohesiveness of the components. On the basis of both the very low build rate and the friability of the components produced this production route was considered not to offer significant scope for the manufacture of bioceramic implants.

3.2. Hydroxyapatite and phosphate glass

Fig. 8 shows scanning electron micrographs of the HA powder alone and the HA powder mixed with 20% phosphate glass. From the image of pure HA it may be observed that the particles exhibit a relatively coarse surface, which could potentially provide a good key for bonding of the phosphate glass as it solidifies. The second image also shows that the phosphate glass appears to be quite evenly distributed among the HA particles, which should provide the sintering mechanisms with a sufficiently interconnected network of melting particles to form a coherent binding structure.

Process charts were developed for increasing proportions of CNP and were seen to produce monolayers across a wide range of parameters (see Fig. 9 for a typical chart). A major problem with all the parts produced, with any combinations of material proportions, scan speeds and laser powers, was the highly friable nature of those layers when handled. This great fragility effectively prevented the removal and inspection of the monolayers, thus negating the possibility of analysing such material before moving on to multiple layer components.

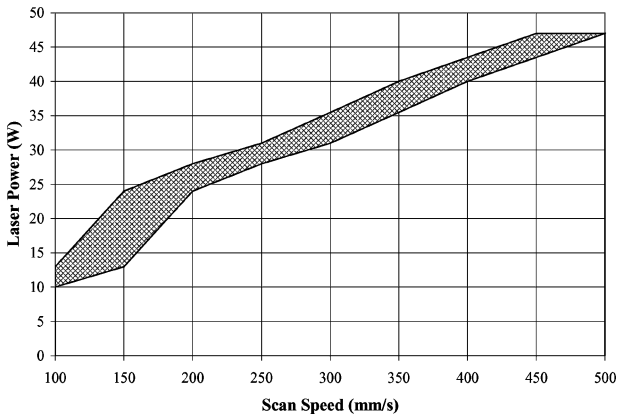

Figure 9 A typical process chart for HA and CNP in a 5% blend (the shaded area indicates successful sintering conditions).

After concluding monolayer scanning for a range of volume fractions, multiple layer construction was undertaken with a powder mixture containing 10% by volume phosphate glass (this was found to be the best compromise between monolayer coherence and the ability to spread the powder) and a layer thickness of 0.25 mm. At speeds of 50 mm/s and above, significant curling of even very small layers of 10×10 mm was observed. "Curl" is a warping phenomena which arises as a result of shrinkage during processing, and which results in nominally flat layers taking on a dish-like shape, with the outer parts of the layer curling up slightly [16]. This led to difficulties in powder spreading as layers which have curled will foul on the spreading mechanism, and so the space between layers had to be increased to take account of the extra depth of the layers. This then led to layers that were too thick, reducing inter-layer bonding and causing unsintered powder to be trapped between layers.

To assess whether or not the multiple layer construction process was at all feasible the scanning speed was reduced to 10 mm/s in an attempt to reduce layer curling. While the first few layers still had a tendency to curl those scanned afterwards exhibited less curl and allowed powder spreading to occur much more reliably, and with a 0.25 mm layer thickness. The multi-layer components produced were, however, quite fragile, as a result of both the poor inter-layer bonding, due to the reasons stated previously, and also intra-layer bonding, in that because of the high degree of porosity of the parts and the thin coating of glass that binds the HA particles together (see Fig. 10).

Those scanned parts that could be removed from the powder bed were examined by SEM, which may be seen in Fig. 11. It may be seen that the general distribution

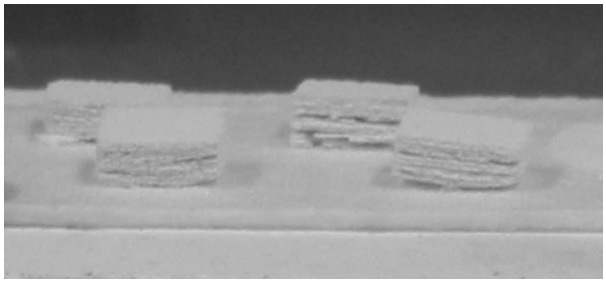

Figure 10 Multilayer components of HA and CNP.

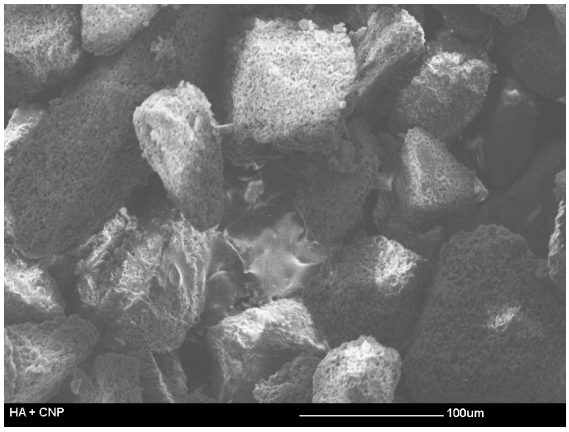

Figure 11 An SEM micrograph of HA and CNP after laser sintering.

of CNP amongst the HA particles that was observed in Fig. 8 has disappeared completely. In its place is an image which shows still discrete HA particles interspersed by occasional, randomly situated pockets of phosphate glass.

This shows that as the CNP particles melted, rather than wetting the surfaces of the HA particles evenly, they have, on the whole, preferentially migrated towards one another, presumably through surface tension effects. This suggests that under these processing conditions the phosphate glass does not have sufficient time to satisfactorily wet the HA particles, as it must in the conventional sintering processes described by Tancred [12]. However, the speed of processing associated with this mixture of glasses means that it offers a far more promising approach to the production of bioceramic implants than processing of A-M glass alone. Future work with this approach will concentrate on developing processing conditions which minimise curl, and which allow for an appropriate amount of phosphate glass and time of laser exposure for the phosphate glass to sufficiently wet the HA.

4. Conclusions

The aim of the work reported in this paper was to investigate the feasibility of using selective laser sintering of glass-ceramic materials to produce bone replacement components. We have concluded that directly sintering A-M glass-ceramics is not feasible as the build rate is so low that the time taken to produce components of any reasonable size would be too long. SLS of an HA/phosphate glass mixture has proven to be the more promising approach, although further work is required to develop more optimal processing conditions and mechanical properties.

Acknowledgments

The research reported in this paper was supported by a University of Leeds studentship. Assistance from N. Bubb (glass preparation), I. Smith (SEM), P. Wood and A. Ismail (sinterstation) is gratefully acknowledged.

References

1. L. L. HENCH and J. WILSON, in "An Introduction to Bioceramics" (World Scientific, Singapore, 1993) p. 1.
2. R. HUISKES, *Acta. Orthop. Scand.* **185** (Suppl.) (1980) 29.
3. P. VINCENZINI, *Mater. Sci. Monogr.* **17** (1983) 3.
4. N. KAY, in "Complications of Total Joint Replacement" (Ballière Tindall, London, 1985).
5. E. BERRY, J. M. BROWN, M. CONNELL, C. M. CRAVEN, N. D. EFFORD, A. RADJENOVIC and M. A. SMITH, *Med. Engng. Phys.* **19** (1997) 90.
6. K. W. DALGARNO and C. S. WRIGHT, *Powder Metall. Progr.* **1** (2001) 70.
7. PADTINC, www.padtinc.com, website accessed on 30/01/2003.
8. J. C. LORRISON, in "Selective Laser Sintering of Bioceramics," PhD Thesis, University of Leeds, Leeds, 2003.
9. C. HAUSER, in "SLS of a Stainless Steel Powder," PhD Thesis, University of Leeds, Leeds, 2003.
10. A. RAVAGLIOLI and A. KRAJEWSKI, in "Bioceramics" (Chapman & Hall, London, 1992) p. 182.
11. A. CLIFFORD and R. HILL, *J. Non-Cryst. Solids* **196** (1996) 346.
12. D. C. TANCRED, B. A. O. MCCORMACK and A. J. CARR, *Biomaterials* **19** (1998) 1735.
13. J. KNOWLES, "Private Communication" (University College London, 2002).
14. M. MICOULAUT, *Eur. Phys. J. B* **1** (1998) 277.
15. R. M. GERMAN, in "Sintering Theory and Practice" (John Wiley and Sons Inc., New York, 1996) p. 226.
16. N. M. JAMAL and K. W. DALGARNO, in Proceedings of the 13th Solid Freeform Fabrication Symposium, Austin, August 2002, edited by D. L.Bourell *et al.* (University of Texas, Austin, 2002) p. 349.

Received 3 December 2003
and accepted 17 December 2004